Materials Today • Volume xxx, Number xx • xxxx 2022

ELSEVIER

The tribovoltaic effect

Shiquan Lin [1,2], Zhong Lin Wang [1,3]

[1] Beijing Institute of Nanoenergy and Nanosystems, Chinese Academy of Sciences, Beijing 100083, PR China
[2] School of Nanoscience and Technology, University of Chinese Academy of Sciences, Beijing 100049, PR China
[3] Georgia Institute of Technology, Atlanta, GA 30332−0245, USA

Contact electrification (or triboelectrification) (CE) is a universal phenomenon between any two materials or two phases of materials. But a contact between two different materials may results in different output. When a p-type semiconductor sliding on a n-type semiconductor surface, the current flowing between the two electrodes on the top of the p-type and the bottom of the n-type is a direct current. This phenomenon is called tribovoltaic effect discovered in the last few years. The mechanism of the tribovoltaic effect is resulted from the electron-hole pairs generated at the PN junction due to the energy released by the formation of the newly formed chemical bonds at the interface due to mechanical sliding, and the inner field built at the PN junction separates the electrons from the holes, resulting in a DC output. The energy released by forming a chemical bond is called "bindington", which serves as the exciton for exciting the electron-hole pairs, in analogy to the photovoltaic effect. Here, we first review the recent works on the tribovoltaic effect observed at different interfaces. Then, the mechanism of the tribovoltaic effect is presented. The surface chemical methods for regulating the tribovoltaic effect are discussed. Finally, a technique of hybrid tribovoltaic nanogenerator based on the tribovoltaic effect and its potential applications are elaborated.

Keywords: Tribovoltaic effect; Semiconductor interface; Bindington

Introduction

As the world enters the era of internet of things (IoTs), the high-entropy distributed energy is urgently needed to power a large number of micro-sensors [1,2]. Triboelectric nanogenerators (TENGs), which were first invented by Wang in 2012, are a typical distributed energy source capable of harvesting mechanical energy from the environment to power sensors [3–10]. Traditional TENGs usually consist of insulators with conductive electrodes [11–14]. When the two insulators contact with each other, the contact electrification (CE) occurs and the insulator surfaces are electric charged. Then, the insulator vibrates against the conductive electrodes driven by mechanical energy, such as human motion [15,16], wind [17,18] and water wave [19,20] *etc.*, generating induced alternating current (AC). Since most micro-sensors require direct current (DC), traditional TENGs are usually equipped with rectifiers, which increase the sizes of the devices and reduces energy harvesting efficiency [21,22]. Recently, the CE and triboelectrification between semiconductors were investigated and it turned out that a DC current will be directly generated when a p-type semiconductor rubbing against a n-type semiconductor, which can be considered as a DC-TENG without rectifier [23–26].

Due to the advantages of DC output, the semiconductor DC-TENG has attracted extensive attention. However, the mechanism of the CE or triboelectrification involving semiconductors has not been clear until the tribovoltaic effect was first proposed by Wang [25]. It was pointed out that the generation of the DC current at the sliding semiconductor interface is similar to the

E-mail address: Lin Wang, Z. (zlwang@gatech.edu)

 https://doi.org/10.1016/j.mattod.2022.11.005

Please cite this article in press as: S. Lin, Z. Lin Wang, Materials Today, (2022), https://doi.org/10.1016/j.mattod.2022.11.005

photovoltaic effect. Once a p-type semiconductor slides on a n-type semiconductor, the newly formed atomic bond at the interface releases an energy quantum, named as "bindington", which excites electron-hole pairs at the PN junction. The electrons and holes are separated by the internal built-in electric field at the PN junction, generating a direct current. This is the tribovoltaic effect, which occurs at PN semiconductor interfaces [27,28] or Schottky junction between a metal and a semiconductor interface [29,30]. The energy quantum, which was named as "bindington", similar to the photon, is introduced here [31–33]. In recent years, the tribovoltaic effect at different interfaces has been widely discussed, and the output of the DC-TENG based on tribovoltaic effect was continuously optimized based on different methods, such as surface modification and material selection, suggesting that tribovoltaic effect has a wide range of potential application in the field of nano energy.

This review provides a summary of recent studies on the tribovoltaic effect. First, the photovoltaic effect and the energy released during friction have been systematically introduced to clarify the mechanism of the tribovoltaic effect at the semiconductor interface. Secondly, the tribovoltaic effect at different interfaces, including metal–semiconductor interface, n-type and p-type semiconductor interface, *etc.*, is reviewed. Third, the surface modification and material optimization methods for improving the tribovoltaic TENG output are systematically summarized. Finally, the contribution of CE to the tribovoltaic effect and the potential applications of the tribovoltaic effect are discussed further.

Mechanisms of tribovoltaic effect

A brief introduction to photovoltaic effect

The tribovoltaic effect is usually analogous to the photovoltaic effect except the source for exciting the electron-hole pair is different. Understanding the photovoltaic effect has significant implications on the tribovoltaic effect. The photovoltaic effect is the physical basis for the conversion of converting light energy into electricity in solar cells, which is an important clean energy source [34–36]. After decades of efforts, the mechanism of the photovoltaic effect is relatively clear compared to the tribovoltaic effect [37–42]. As shown in Fig. 1, photovoltaic cells are usually composed of different semiconductors. Fig. 1a gives the band structure of p-type and n-type semiconductors before contact. When the n-type semiconductor contacts the p-type semiconductor, the majority carrier in n-type semiconductor (electron) will diffuse to the p-type semiconductor side, and the hole will diffuse from the p-type semiconductor side to the n-type semiconductor side, until the Fermi level of the two semiconductors reaches equilibrium, and a built-in electric field is established. Then, the incident photon provides the energy to excite the electron-hole pairs (Fig. 1b), which is further separated under the built-in electric field (Fig. 1c), realizing the conversion of light energy to electric energy.

Photovoltaic cells have been successful in the field of clean energy and are now an important means of harvesting clean energy. The tribovoltaic effect is similar to the photovoltaic effect, the only difference is that the tribovoltaic cell converts mechanical energy into electrical energy, instead of light energy to electric energy. And the tribovoltaic cell is complementary to the photovoltaic cell and is expected to become another important way to obtain clean energy.

Bonding and energy releasing during contact electrification

Unlike the photovoltaic effect, the energy to excite the electron-hole pairs at the interface in the tribovoltaic effect comes from friction. How friction excites electron-hole pairs at the interface is a key to understand the tribovoltaic effect. Friction is the resistance caused by the interaction between the two sliding contact surfaces, which occurs at almost any sliding interface with energy loss [41–46]. It can be considered that tribovoltaic effect converts part of the dissipated energy during friction into electrical energy. The energy dissipation in friction is a complicated topic, which has been discussed for a long time. At macroscale, frictional force is proportional to the normal load, which is often called Coulomb's law [45,46]. Different friction theory was proposed to explain the Coulomb's law, such as the mechanical engagement theory, in which the friction originated from surface roughness, and the frictional energy is loss in roughness engagement, collision and plastic deformation, such as plowing through the hard asperities to embed in the soft surface [47,48]. The adhesion effect in friction was also considered, which points out that the friction may come from the adhesion of two asperities at the interface due to the dramatic temperature

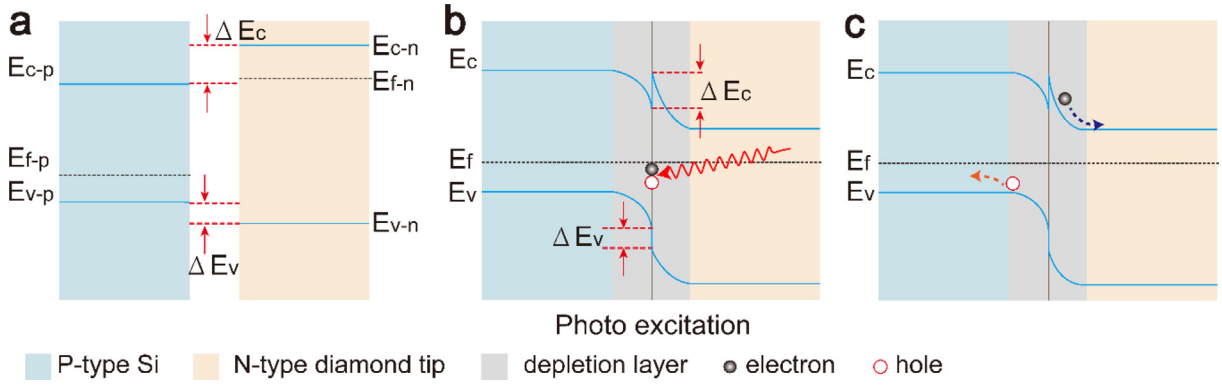

FIGURE 1

Energy band diagram of the photovoltaic effect. (a) Energy band diagram of the p-type and n-type semiconductors before contact. (b) Energy band diagram of the P—N junction and photoexcitatatoin of electron-hole pairs. (c) Seperation of electron-hole pairs under built-in electric field [69].

Please cite this article in press as: S. Lin, Z. Lin Wang, Materials Today, (2022), https://doi.org/10.1016/j.mattod.2022.11.005

increase at microscale [49,50]. We can conclude from the macroscopic friction theory that the energy lost in friction is converted into heat and deformation energy. The deformation of the materials is unlikely to excite the electron-hole pairs at the interface, but the temperature rise is a potential factor for excitation of the electron-hole pairs, which was discussed by using quantum mechanical calculations [51].

It was demonstrated that the tribovoltaic effect can occur at a super-lubricated interface [52], in which the deformation of materials is limited. It also suggests that the deformation of materials cannot be the factor that excites the electron-hole pairs at the interface, and the energy dissipation in the friction should be discussed at atomic scale to understand the generation of tribovoltaic effect. It has been shown that the friction does not completely disappear and is sometimes even significant at the atomic flat crystal surface, and the various micro-friction theories were proposed, such as "cobblestone" model [53,54], oscillator model [55,56], phonon friction model [57] and bond formation model [58–64]. In these models, the energy is dissipated in the form of atomic vibrations and chemical bond formation, in which the energy released by bond formation could be large enough to excite the electron-hole pairs. As shown in Fig. 2, some of the silicon atoms are terminated by a –OH group [59]. During sliding, the –OH group forms a siloxane bond (Si-O-Si) with another –OH group on the other surface through the silanol condensation reaction, and releases a H_2O molecule [63,64]. On the other hand, the some formed siloxane bonds are torn, absorbing energy, causing mechanical energy lost and generating friction force [65]. As the sliding continues, the siloxane bonds are constantly being formed and broken, the formation of the chemical bonds will release an energy quantum, which was named as "bindington". The energy value of the "bindington" depends on the energy difference between the orbitals of the electron before and after the bonding, which could be up to several electron volts. Several electron volts energy is enough to excite an electro-hole pair at least at the semiconductor interface [31,32]. In this process, the formation and broken of the chemical bonds can be considered as a pump to convert the mechanical energy into electricity. In fact, the friction process is very complex, and the current experimental studies on the tribovoltaic effect have not discussed the friction process in depth, which is a key issue in future research on the tribovoltaic effect. But anyway, the formation of chemical bonds could be an important energy source for the excitation of electrons.

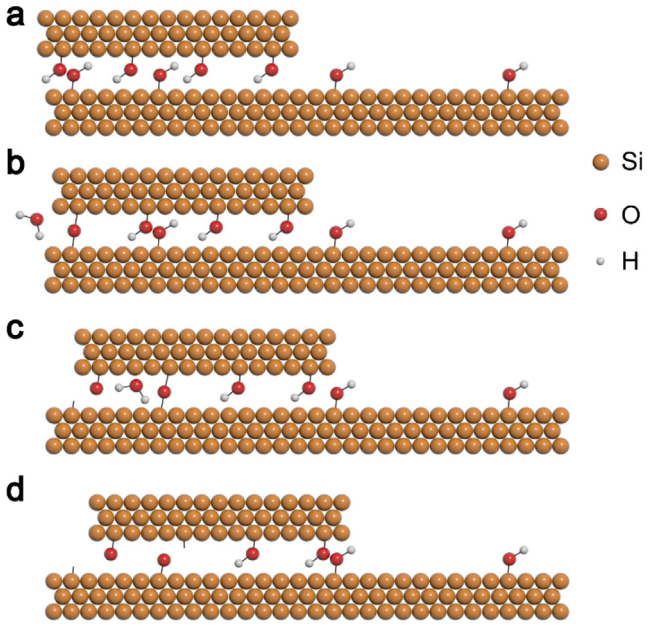

FIGURE 2

Schematic of the chemical reactions at a sliding silicon interface in which the formation of chemical bonds occurs.

In general, phonons can be excited locally at the interface during materials sliding due to local elastic and possibly plastic deformation. But we believe that the phonon energy in the range of 10–50 meV is not enough to excite electron-hole pairs an PN junction, which usually requires an energy more than 1.1 eV to be excited as for silicon. At low-sliding speed, local heating may not a problem, but at a high speed of sliding, local heating could be more serious. In this case, the situation could be more complex.

Friction produced DC current during sliding-mode tribovoltaic effect

Based on the above discussion, the tribovoltaic effect can be described clearly analogous to the photovoltaic effect, and we emphasize the role of the energy release by the formation of chemical bonds at the interface. Fig. 3a gives the energy band diagram of p-type semiconductor and n-type conductor in contact. When the two semiconductors contact each other, the electron will diffuse from n-type semiconductor side to the p-type semiconductor side, while the holes diffuse from p-type semiconductor side to the n-type semiconductor side, hence forming a built-in electric field, to compensate the difference in the Fermi level. On the surface of the semiconductor, the periodic arrangement of atoms is terminated with dangling bonds on the surface atoms. When there is a relative motion between the upper and lower surfaces, the distance between the atoms belonging to the two surfaces changes. If the distance of the atoms gets close enough, the dangling bonds will interaction with each other, further forming a new chemical bonds, and release an energy quntum ("bindington") (Fig. 3b), because forming a bond is energetically favorable in a general case. The "bindington" plays the role of incident photon in the photovoltaic effect, exciting the electron-hole pairs at the interface (Fig. 3c). And then, the electron-hole pairs are separated under the built-in electric field, and the electron transfer to the n-type semiconductor side, while the hole transfer to the p-type semiconductor side (Fig. 3c), so that the direction of the tribo-current is from p-type semiconductor side to the n-type semiconductor side in the external circuit. And it needs to be mentioned that the formed chemical bonds between the atoms will be torn by the mechanical force, as the relative motion of the two surfaces continues, which is a process of adsorbing energy, conversing the mechanical energy to the chemical energy, and generating friction force. The whole process of the tribovoltaic effect is shown in Movie 1. The relationship between photovoltaic effect and tribovoltaic effect can be simply illustrated in Fig. 3d. It is shown that the only difference

Please cite this article in press as: S. Lin, Z. Lin Wang, Materials Today, (2022), https://doi.org/10.1016/j.mattod.2022.11.005

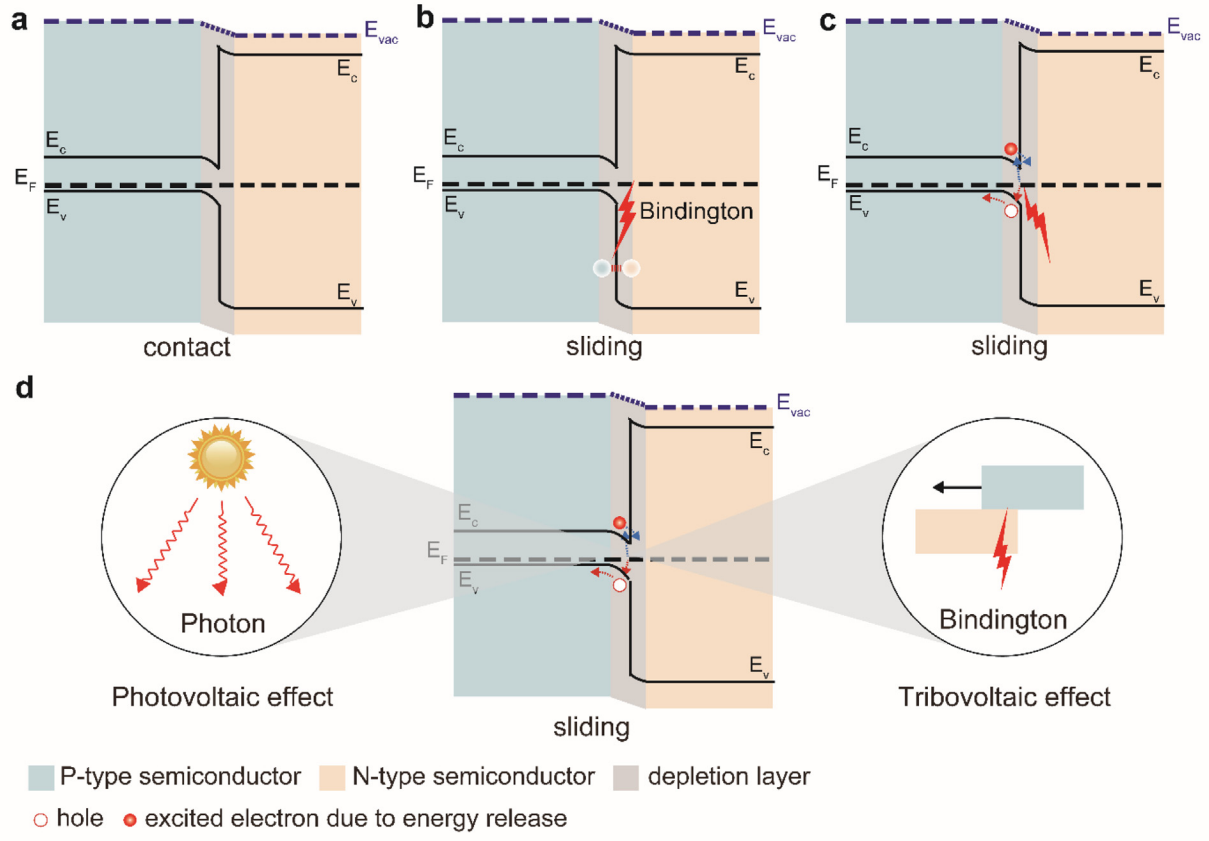

FIGURE 3

Energy band disgram of the tribovoltaic effect. Energy band diagram of the p-type semiconductor and the n-type semiconducotr (a) in contact and (b) in sliding. (c) The movement of the electrons and the holes at the p-type semiconductor and p-type semiconductor interface in sliding. (d) The illustration of the relation between photovaltaic effect and tribovoltaic effect. (E_c is the bottom of the conduction band, E_f is the Fermi level of the semiconductors, and E_v is the top of the valence band.).

between the two is the source of energy that excites the electron-hole pairs.

It is important to note that although we used the term of tribo- in tribovoltaic effect, in physics, there is no need to rub one material against another, but a physical contact at a separation at sub-Angstrom scale is enough for generating the effect. Since tribo- is more familiar to people, we use tribo- instead of contacting. Moreover, in current tribovoltaic effect theory, the band diagram of the two semiconductors in contact mode and that in sliding mode is considered as the same for simplicity, that is, no study has considered the influence of sliding on the structure of band diagram. In fact, sliding is highly suspected to affect the band diagram of two semiconductor surfaces, since in the initial contact, both surfaces are virgin surfaces without carrier diffusion, and during sliding, one surface is virgin and the other one is with the diffused carrier from previous contact. This effect is subject to further discussion.

Tribovoltaic effect at different interfaces

The conditions for the tribovoltaic effect are the presence of a built-in electric field at the interface and the electron-hole pairs excited at the frictional interface. The temperature rises and formation of chemical bonds at sliding interfaces are universal phenomena that occur at almost any frictional interface, which implies that any sliding interface with a built-in electric field should have a tribovoltaic effect. As expected, recent studies have demonstrated that the tribovoltaic effect can occur at various interfaces, including metal–semiconductor interface (Schottky junction) [24,68–73], P—N junction [69,74–76], metal–insula tor-semiconductor interface [72,77–81], metal–insulator-metal interface [80] and even liquid-semiconductor interface [31,32,83–87], as shown in Fig. 4.

Metal-semiconductor interface

Before the tribovoltaic effect at metal–semiconductor interface was first proposed by Wang [25], Shao *et al*. used a metal electrode to contact the conducting polymers without lateral friction, such as poly-pyrrole (PPy) [66]. They noticed that the electrons excited by mechanical power could tunnel though a Schottky junction to generate DC current. The development of tribovoltaic effect was facilitated by the atomic force microscopy (AFM). By using a conductive tip or a semiconductor tip to rub a semiconductor sample, the tribo-current can be recorded by the conductive atomic force microscopy (CAFM) mode, and the tribo-voltage can be obtained by applying a compensating voltage to eliminate the tribo-current. Moreover, the rectifying characteristics of the interface can be measured via current–voltage (I-V) experiments by using AFM equipment. The conductive AFM

Please cite this article in press as: S. Lin, Z. Lin Wang, Materials Today, (2022), https://doi.org/10.1016/j.mattod.2022.11.005

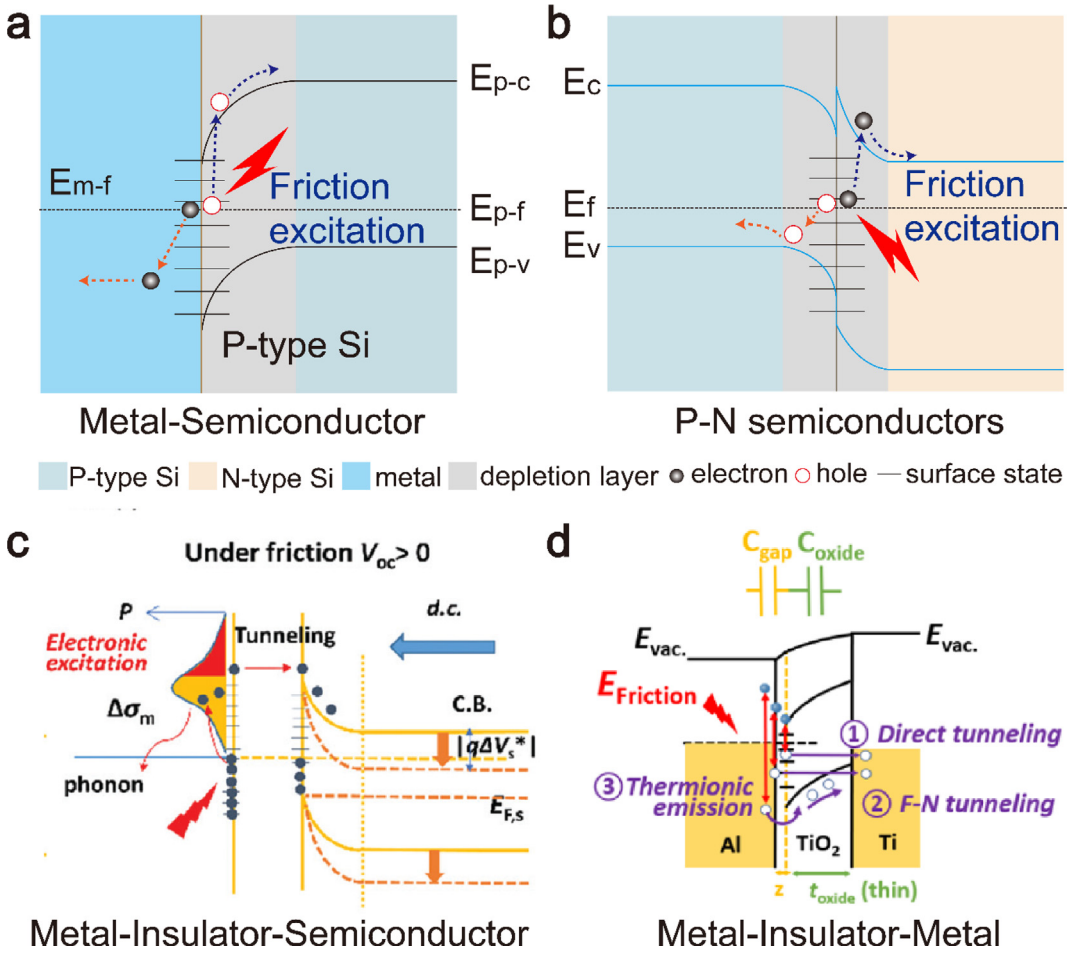

FIGURE 4

Tribovoltaic effect at different interfaces. (a) Metal-semiconductor interface. (b) P—N junction [69]. (c) Metal-insulator-semiconductor structure [76]. (d) Metal-insulator–metal structure [80].

tip has lower resistance compared to the semiconductor AFM tip, and the conductive tip is also easier to obtain than specifically doped semiconductor tips. So that the study of tribovoltaic effect at microscale starts from the metal–semiconductor interface (Schottky junction, Fig. 4a). Liu *et al*. used a Pt-coated silicon AFM tip to rub over a molybdenum disulfide (MoS_2), generating a continuous DC current with a maximum density of 10^6 A/m^{-2}(−|-), which is much larger than most traditional TENGs [24]. The I-V experiments suggested that there was a Schottky barrier at the Pt-coated tip and MoS_2 interface. Combining finite element simulation, Liu *et al*. proposed that the tribo-current is induced by electronic excitation under friction, and the rectifying Schottky barrier at the interface plays a critical role. This explanation is very close to the tribovoltaic effect, but the concept of the tribovoltaic effect was not clearly established. In order to avoid the effect of wear of the metal-coated tip on the tribovoltaic effect at metal–semiconductor interface, Zheng *et al*. use a pure Pt tip to rub both the p-type and n-type silicon samples, and the direction of the tribo-current is from p-type silicon side to the Pt tip side and from Pt tip side to the n-type silicon side in the external circuit, which is consistent with the tribovoltaic effect [69]. Some DC-TENGs based on tribovoltaic effect at metal–semiconductor interface were designed [71]. One advantage of these DC-TENG compared to that based on tribovoltaic effect at P—N junction is that the metals have a lower resistance, which corresponds to a lower internal resistance.

P—N semiconductors interface

Similar to the tribovoltaic effect at metal–semiconductor interface, the DC current can be also generated at a P—N junction (Fig. 4b). Before discussing the tribovoltaic effect at a P—N junction, it is worth mentioning the work on the contact electrification between n-type silicon and p-type silicon. Zhang *et al*. used a n-type silicon to contact a p-type silicon without friction, and the current between the two silicon samples was recorded [74]. It was found that the direction of the contact current was related to the chemical potential difference between the two silicon samples. The Fermi level of n-type silicon is usually higher than that of p-type silicon. When they come into contact, the electrons will transfer from the n-type silicon surface to the p-type silicon surface. When they separate, the transferred electrons will transfer back from the p-type silicon to the n-type silicon in the external circuit, generating current. Further, Xu *et al*. used n-type silicon to rub a p-type silicon in macroscale, and the DC current was generated between the two sliding silicons. In this case, the direction of the DC current was from p-type silicon to the n-type

Please cite this article in press as: S. Lin, Z. Lin Wang, Materials Today, (2022), https://doi.org/10.1016/j.mattod.2022.11.005

silicon in the external circuit, which is consistent with the direction of the built-in electric fields at the P—N junction, suggesting that the tribo-current is caused by the tribovoltaic effect [73]. In microscale, Zheng *et al*. used a n-type diamond-coated silicon tip to scan both the p-type silicon and n-type silicon with different doping concentrations by using CAFM [69]. It was revealed that the tribo-current can be generated at the n-type tip and p-type silicon interface but not at the n-type tip and n-type silicon interface, and the direction of the current is from p-type silicon to the diamond-coated tip in the external circuit. Moreover, I-V tests have shown that the current between the diamond-coated tip and p-type silicon samples is highly dependent on the rectifying characteristics of the tip and sample interface. The stronger the rectification characteristics of the interface, the larger the tribo-current. All these observations support that the tribovoltaic effect occurs at the P—N junction.

Metal-insulator-semiconductor structure

When a metal contacts a semiconductor directly, the Schottky barrier will be established and the excited electrons have been demonstrated to be able to tunnel through the Schottky barrier. As we know that electrons have a tunneling effect, it was wondered that if there is an insulator layer between a metal and a semiconductor, can the friction excited electrons pass through the interface. Liu *et al*. used a conductive tip to slide against a silicon oxide layer with a thickness of 1 ~ 2 nm on the silicon wafer [79]. It was found that the friction excited electrons can tunnel though the oxide layer, generating a DC tribo-current (Fig. 4c). And the tribo-current was 2 ~ 3 orders higher than the dielectric AC output in the traditional TENGs, up to 35 $A/m^{-2}(-|-)$. However, the output of the metal-SiO_x-Si tribovoltaic nanogenerator is highly dependent on the thickness of the oxide layer, which is expected as the tunneling distance of the electrons is limited. If the thickness of the insulator layer increases, the resistance of the metal-SiO_x-Si structure will increase dramatically. Deng *et al*. rubbed a silicon by using a conductive tip to investigate the tribovoltaic effect at a Schottky junction [77]. They noticed that the tribovoltaic current degraded with the increasing of the scan cycles. It was suggested that the degradation of the tribo-current was caused by the formation of the silicon oxide layer induced by the built-in electric field and adsorbed water molecules at the tip and sample interface. Experiments showed that the tribo-current was close to zero after five scans, which implies that the silicon oxide layer was too thick for electrons to tunnel through. In some metal–insulator-semiconductor systems, the current can be generated when the thickness of the insulator layer up to 200 nm, which is explained by thermionic emission and defect conduction theory [76].

Based on current studies, the tribo-current at the metal–semiconductor interface is usually larger than that at the metal–insulator-semiconductor interface due to the higher resistance in the metal–insulator-semiconductor structure. However, it was reported that the output voltage of the metal–insulator-semiconductor sliding generator is usually higher than that of the metal–semiconductor sliding generator, which is attributed to the enhanced barrier height and charged/discharged of the hot electrons at the interface [72]. Moreover, the tribovoltaic effect highly depends on the interaction of two surfaces since that the electron-hole pairs in tribovoltaic effect are excited by friction. As we know, the surface of an insulator is different from the surface of a conductor, such as the surface thermal conductivity, *etc*. So that the interaction between the conductor and some insulators may be stronger than that between two conductors, exciting more electrons and generating a higher tribo-current/tribo-voltage. Therefore, introducing a thin insulator layer in at the metal–semiconductor interface is an effective method to optimize the tribovoltaic nanogenerator.

Metal-insulator–metal structure

For the metal–insulator-metal structure, Benner *et al*. investigated the DC output characteristics of Al-TiO_2-Ti and Al-Al_2O_3-Ti heterojunctions [80]. It was found that the open-circuit voltage of the Al- TiO_2-Ti generator increased from −0.03 to −0.52 V as the thickness of TiO_2 increased from 0 to 200 nm in the case of vertical configurations, which means that out-of-plane carrier transport through the interfacial layer. While the short-circuit current initial increased with the increasing of the thickness of TiO_2, reached its peak value at 20 nm thickness, and then decreased with the increasing of the thickness. The I-V characterization shown that the DC output of the Al- TiO_2-Ti generator depended on both the voltage and resistance of the structure, in which the both increased with increasing insulator thickness. It was proposed that quantum tunneling, thermionic emission and trap-assisted transport contributed to the tribo-current (Fig. 4d), in which the quantum tunneling paly dominated role with thin insulator thickness, and the main charge transfer mechanism switched to thermionic emission/trap-assisted transport when the insulator layer was thick. This work proved that both the tribovoltaic effect and capacitive effect contribute to the DC current generation of the sliding metal–insulator-metal structure.

Liquid-semiconductor interface

Recently, the contact electrification between liquid and solid has attracted extensive concern, owing to the invention of liquid–solid TENG and its potential impacts on the chemical reactions [20,88–98]. Similar to contact electrification, the tribovoltaic effect not only occurs at solid–solid interface, but also at liquid–solid interface. Lin *et al*. designed experiments to investigate the tribovoltaic effect at aqueous solution and silicon interface, in which a syringe conductive needle was used to drag a DI water droplet to slide over a silicon wafer surface, and the tribo-current and tribo-voltage were recorded, as shown in Fig. 5a [85]. It was found that a DC tribo-current can be generated during the sliding, as shown in Fig. 5b. The direction of the tribo-current was from p-type silicon to the aqueous solution or from aqueous solution to the n-type silicon in the external circuit, implying that the electrons moved from p-type silicon side to the aqueous solution side or from n-type silicon side to the aqueous solution side at the interface. Combining I-V characterizations, the direction of the tribo-current at the sliding aqueous solution-silicon interface was found to be the same with the direction of the built-in electric field at the interface, which was consistent with the tribovoltaic effect. Further, the liquid–solid sliding experiments were performed under light irradiation [32], the results shown that the tribo-current between aqueous solution and sili-

Please cite this article in press as: S. Lin, Z. Lin Wang, Materials Today, (2022), https://doi.org/10.1016/j.mattod.2022.11.005

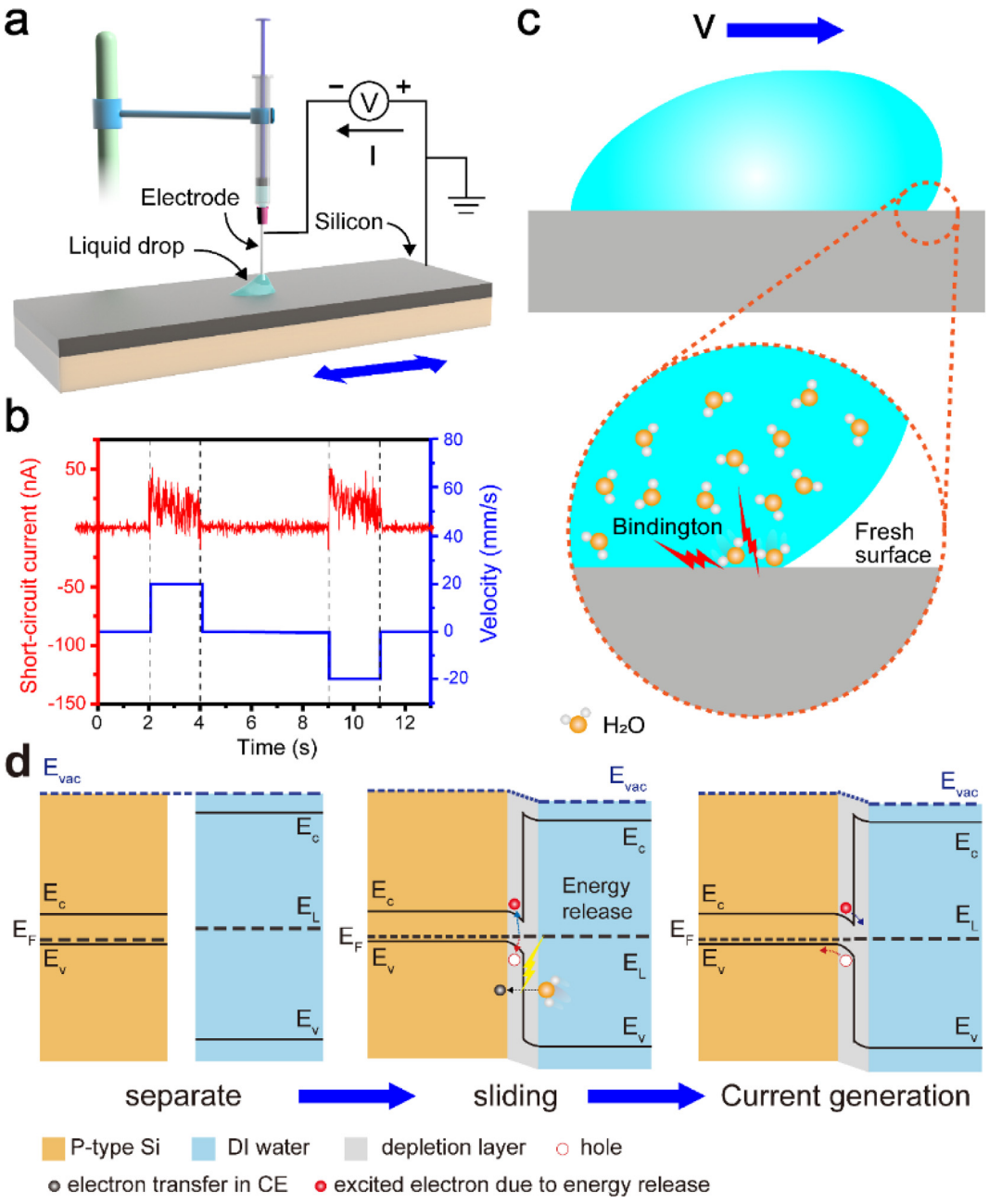

FIGURE 5

Tribovoltaic effect at the liquid-semiconductor interface. (a) The setup of the tribovoltaic experiments and the external circuit [85]. (b) The oscillogram of tribo-current when a DI water droplet slides on the p-type silicon wafer. (c) The generation of the "bindington" at the sliding water and semiconductor interface [33]. (d) Energy band diagram of the tribovoltaic effect at a liquid–solid junction.

con wafer can be enhanced by the light irradiation, owing to the increasing of the electro-hole pairs at the interface, also supporitng that tribovoltaic effect occurs at liquid–solid interface.

A key point in understanding the tribovoltaic effect at the aqueous solution-semiconductor interface is that the aqueous solution can be considered as a liquid semiconductor [97–102]. When the aqueous solution contacts the solid semiconductor, the electrons will diffuse from one surface to the other surface to establish the built-in electric field, as that occurs in the P—N junction. During sliding, the aqueous droplet will contact the fresh surface of the solid semiconductor, forming new chemical bonds and releasing energy quantums (was named as "bindingtons"), as shown in Fig. 5c. The temperature effect on the tribovoltaic current supported the generation of "bindingtons" [31]. It was revealed that the tribovoltaic current between aqueous solution and solid semiconductor increased with the increasing temperature, which was caused by more violent collisions between water molecules and solid surface, resulting in the release of more "bindingtons". Analogous to the tribovoltaic effect at the solid–solid interface, the whole process of the tribovoltaic effect at the liquid–solid interface can be described, as shown in Fig. 5d. First, there is a built-in electric field at the liquid–solid interface

Please cite this article in press as: S. Lin, Z. Lin Wang, Materials Today, (2022), https://doi.org/10.1016/j.mattod.2022.11.005

due to the diffusion of electrons driven by the difference in the Fermi levels. During sliding, the "bindington" will be released to excite electron-hole pairs at the interface, and then the electron-hole pairs are separated by the built-in electric field, generating a DC current.

Here, we designed a table to compare the mechanisms and output performance of the tribovoltaic effect at different interfaces for a better understanding, as shown in Table 1. It should be noticed that this is a qualitative table. Because there is no standard test method in the study of tribovoltaic effect, the experimental conditions are different for the data, so it is impossible to make a quantitative comparison currently.

Interfacial engineering for enhanced tribovoltaic effect

Development of high-performance DC nanogenerators based on the tribovoltaic effect is a key topic in the academic community. The output tribovoltaic current and voltage are demonstrated to be highly dependent on the interfacial properties of the tribovoltaic nanogenerator. It was reported that the real contact area, load and the density of surface states of the semiconductor can significantly affect the tribovoltaic effect. Therefore, it is an important way to improve the output of tribovoltaic nanogenerators by changing the surface properties of the semiconductors.

Surface states enhancement

Surface states can be understood as the position on the surface that holds electrons, which is generated due to the termination of periodic arrangement of atoms on the surface. Theoretically, the density of surface states of the semiconductor may affect the tribovoltaic effect from three aspects. First, the electrons in the surface states are easier to be excited than those in the valence band, as less energy is required. The higher the density of surface states, the larger the number of electrons can be held on the surface, and more electrons can be excited, generating more electron-hole pairs, and increasing the tribovoltaic current. Secondly, a higher surface states density corresponding to more dandling bond on the surface, resulting in more chemical bonds formation during sliding, releasing more "bindington". Third, the surface states density of semiconductors can affect the interface band structure and the strength of the built-in electric field, and further tribovoltaic current and voltage.

Zheng *et al*. used inductively coupled plasma reactive ion etching (ICP-RIE) method to enhance the density of surface states of the silicon, and tested the tribovoltaic effect between two semiconductors before and after the ICP-RIE treatment, as shown in Fig. 6a [69]. The results turned out that the tribovoltaic current between the tip and the treated semiconductors increased dramatically, as shown in Fig. 6b and 6c. The I-V characterizations implied that the built-in electric field at the semiconductor interfaces was not enhanced by the ICP-RIE treatment of the semiconductors. While the X-ray photoelectron spectrums (XPS) suggested the adsorbing of fluorine and sulfur elements on the Si sample surfaces, which may introduce new surface states. On the other hand, the ICP-RIE treatment may produce defects on the surface, which may also increase the density of surface states of the Si samples. From these results, it can be concluded that the tribovoltaic effect can be enhanced by increasing the density of surface states of semiconductors, and some works about the dynamic Schottky generator also supported this conclusion [70].

At a solid–solid interface, the real contact area is much less than the nominal contact area due to the existence of rough asperities. Increasing the real contact area, letting more surface states of the semiconductor to be involved in friction is another sense of increasing the surface states density. An effective way to increase the real contact area is to choose flexible materials in contact. For example, there are a large number of nano-sized protrusions on the flexible carbon aerogel surface, which increases the real contact area at the interface. Therefore, the carbon aerogel-SiO_2-Si tribovoltaic nanogenerator has a high output performance (Fig. 6d) [101].

Interfacial electric field enhancement

The excited electron-hole pairs are separated by the built-in electric field in tribovoltaic effect. A stronger built-in electric field separates electron-hole pairs more efficiently. The Fermi level difference between the two semiconductors before contact is an important factor that can affect the strength of the built-in electric field at the interface. It was reported that the tribovoltaic current and voltage between diamond tip and silicon sample highly depended on the doping concentration of the silicon sample, which affects the Fermi level of the silicon [69]. The doping concentration of silicon sample also affects the tribovoltaic effect at liquid-semiconductor interface [85]. Experiments have shown that the tribovoltaic current and voltage at the aqueous solution-silicon also increased with the doping concentration of silicon in a certain range. Therefore, it is an important method to optimize the tribovoltaic nanogenerator by selecting the appropriate semiconductor doping concentration to establish a relative strong interfacial built-in electric field. As discussed in Section 3.3, introducing an insulator layer at the semiconductor interface is another way to enhance the built-in electric field and the interface barrier higher, and further enhance the output performance of the tribovoltaic nanogenerator [76].

TABLE 1

The tribovoltaic effect at different interfaces.

	Friction excitation	Tunneling of electrons	Internal resistance	Output voltage	Output current
Metal-semiciondoctor	Yes	No	Low	Low	High
P—N junction	Yes	No	Middle	Middle	Middle
Metal-insulator-semiconductor	Yes	Yes	High	High	Middle
Metal-insulator–metal	Yes	Yes	Middle	Middle	Middle
Liquid-semiconductor	Yes	No	Middle	Middle	Middle

Please cite this article in press as: S. Lin, Z. Lin Wang, Materials Today, (2022), https://doi.org/10.1016/j.mattod.2022.11.005

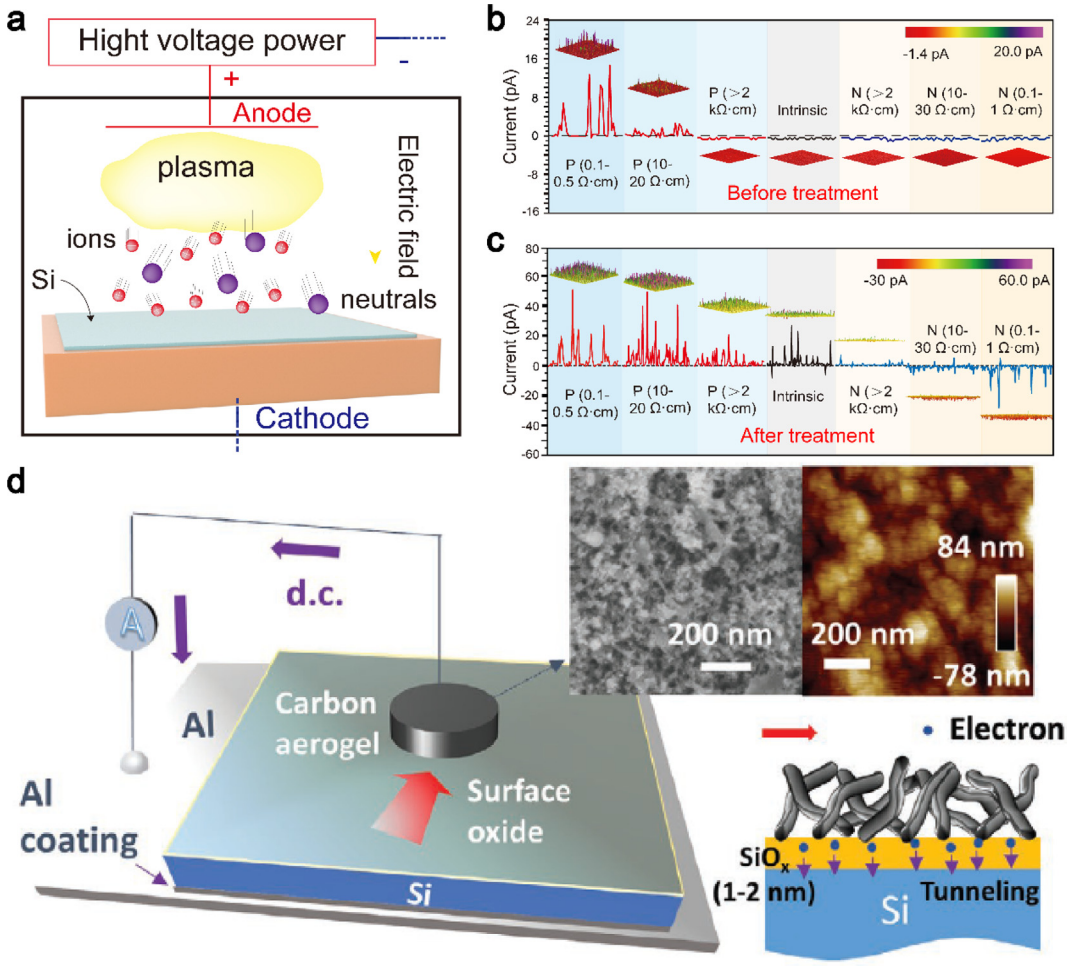

FIGURE 6

Effect of the surface states density of the semiconductor and the contact area on the tribovoltaic effect. (a) The setup of the ICP-RIE treatment for enhancing the surface states density of the silicon. The tribovoltaic current between a n-type tip and the silicon samples (b) before ICP-RIE treatment, (c) after ICP-RIE treatment [69]. (d) The tribovoltaic effect at the SiO_2 (with oxide layer) and carbon aerogel [101].

Surface chemistry on tribovoltaic effect

Surface functional groups play an important role in many effects, especially those related to friction, such as contact electrification and tribovoltiac effect. It was demonstrated that the surface functionalization is an effective method for tunning the output performance of the tribovoltaic nanogenerator [102,103]. The surface work function of the semiconductors, which is very sensitive to the surface functional group, can be regulated by surface modification, and then the barrier height and built-in electric field strength at the interface of semiconductors can be controlled, further affecting the tribovoltaic effect. Moreover, as proposed in Section 2.3, the energy to excite electron-hole pairs is released by the formation of chemical bonds during friction. The energy of the released "bindington" depends on the functional groups on the two sliding surfaces and what chemical bonds form at the interface. Selecting functional groups with high chemical energy can help to release high energy "bindington" during friction and improve the output performance of tribovoltaic nanogenerator.

Ferrie *et al*. grafted organic mobolayers bearing a range of terminal functional groups on silicon surface by means of hydrosilylation chemistry (Fig. 7a) [104,105]. And the tribovoltaic effect between the functionalized silicon and Pt tip was investigated by using CAFM (Fig. 7b). It turned out that the tribo-current between the Pt tip and the monolayer functionalzed silicon was significantly affected by the terminated functional groups of the monolayer. The effect of work function, adhesion, wettability of the functionalized surface on the tribovoltaic effect was discussed. This work bridges the field of surface chemistry and molecular electronics, which for the first time demonstrated the effect of surface chemical functional groups on the tribovoltaic effect. But the formation of chemical bonds at the interface was not mentioned in this work. According to the mechanism of the tribovoltaic effect, the control of interface bonding is one of the ideas for surface chemistry in the tribovoltaic effect.

Super-lubricated interface

A tribovoltaic nanogenerator converts mechanical energy into electrical energy through friction. Unfortunately, mechanical energy is also converted into other energies during friction, such as deformation energy and thermal energy, and even only a

Please cite this article in press as: S. Lin, Z. Lin Wang, Materials Today, (2022), https://doi.org/10.1016/j.mattod.2022.11.005

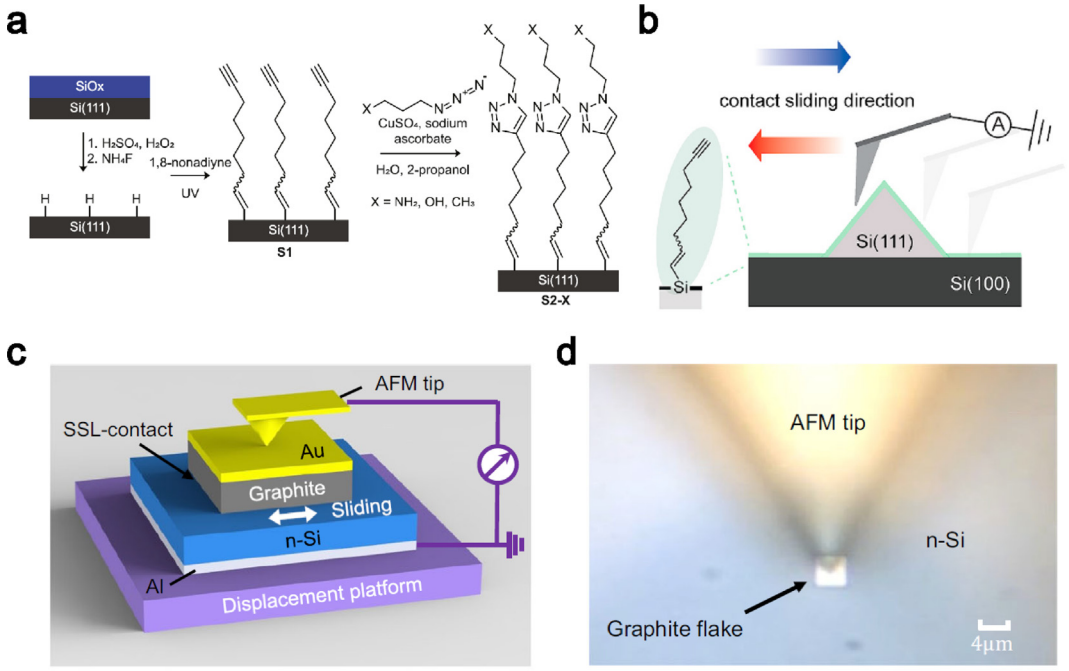

FIGURE 7

Surface chemistry and superlubrication in the tribovoltaic effect. (a) Schemetics of the surface functionalization of the silicon sample, and (b) schematics of the CAFM experiment [104,105]. (c) Structure of a graphite-silicon tribovoltaic nanogenerator, and (d) optical microscopic image of a graphite-silicon tribovoltaic nanogenerator [52].

small part of it can be converted into electricity, making tribovoltaic nanogenerator inefficient. On the other hand, semiconductor wear also leads to poor stability of the tribovoltaic nanogenerator. Therefore, reducing the friction contributed by the plowing effect and plastic deformation, further reducing the wear and frictional coefficient, can improve the energy conversion efficiency of the tribovoltaic nanogenerator.

Yang *et al*. designed a new tribological-behavior-controlled DC triboelectric nanogenerator (TCDC-TENG) by introducing a lubricating layer (polyalphaolefin SpectraSyn 4, PAO 4) on the semiconductor surface [106]. It was demonstrated that the TCDC-TENG can generate a stable DC output even in a high load and high sliding speed without significant wear. And the output was found to increase with increasing load and sliding speed. Zhang *et al*. used the graphite-like carbon (GLC) and polytetrafluoroethylene (PTFE) as the lubricating layer, and the friction coefficient of the macroscale tribovoltaic nanogenerator was reduced to less than 0.01 [107]. Meanwhile, the current and power density of the super-lubric tribovoltaic nanogenerator reached 60nA and 5.815 W/m^2, respectively.

In microscale, Huang *et al*. used a conductive AFM tip to press on the top of a graphite flake, and controlled it to slide on an atomic smooth surface of n-type silicon (Fig. 7c and 7d) [52]. During sliding, the friction force between the graphite flake and silicon was measured by using lateral force microscopy while the tribo-current was recorded by using CAFM. The micro tribovoltaic generator made of graphite flake and silicon has an output of 210 A/m^{-2}(−|-) and a power density of up to 7 W m^{-2}, while friction coefficient is less than 0.01. These super-lubric tribovoltaic generators maintain good output performance while significantly reducing friction. The small friction force means that very little mechanical energy is needed to drive the generator, increasing the efficiency of converting mechanical energy into electricity.

Material engineering for tribovoltaic effect

As discussed above, the most commonly used semiconductor material for tribovoltaic effect studies is silicon, which is already widely used and has a well-established fabrication process. Silicon is very well understood, so a study of the tribovoltaic effect of silicon material can better discuss the mechanism. However, the silicon-based tribovoltaic nanogenerator also has some drawbacks. On the one hand, its output performance is not very high. On the other hand, due to the mechanical properties of silicon, such as its relatively brittle and hard nature, it cannot be directly used on many occasions, especially those that require interaction with humans.

Therefore, special materials were designed for the production of tribovoltaic nanogenerators, which improved the output performance of tribovoltaic nanogenerators and also allowed the nanogenerator to be used on some special occasions.

Flexible and organic materials

Flexible wearable devices have developed rapidly in recent years [108–112]. Harvesting the mechanical energy of human motions directly to power a wearable device is a perfect strategy. Therefore, it is of great significance to study the tribovoltaic effect of flexible materials and design flexible tribovoltaic nanogenerators. Yang *et al*. investigated the tribovoltaic effect at sliding metal-conducting polymer interfaces. In the experiments, different metals were used, such as Al, Cu, Fe, Au and Pt [111]. The PEDOT:PSS supported on flexible PDMS was chosen as the con-

Please cite this article in press as: S. Lin, Z. Lin Wang, Materials Today, (2022), https://doi.org/10.1016/j.mattod.2022.11.005

ducting polymer. It was found that the tribovoltaic voltage highly depended on the work function difference between the metal and the conducting polymers, and the highest output current of 20 A/m^{-2}(−|-) and open circuit voltage of 0.8 V were achieved at the Al-PEDOT:PSS interface. In addition, You *et al.* used the Al alloy, Si, ITO, Cu and graphene to slide against the PEDOT:PSS surface and discussed the tribovoltaic effect at the flexible materials interface [112]. It was also found that the optimal output was the tribovoltaic nanogenerator composed of PEDOT:PSS and Al alloy, which achieved short-circuit current up to 309 μA, and open-circuit voltage up to 1 V.

Above two works proved that the tribovoltaic effect occurs at sliding metal and flexible conductive polymer interfaces. Based on this phenomenon, Meng et al. designed a textile tribovoltaic DC nanogenerator, which is a big step towards the application of flexible tribovoltaic nanogenerators [113]. As shown in Fig. 8a, the conducting polymer PEDOT was coated on the conductive Ni-coated textile substrate, which was chosen as an electrode. When a metal, such as Al foil slid on the PEDOT coated textile substrate, a DC current was generated (Fig. 8b). Fig. 8c and 8d give the electricity generation process of the textile tribovoltaic nanogenerator. When the Al foil contacts the PEDOT coated textile, the electron in the Fermi level of Al will transfer to the lower empty energy levels of PEDOT, establishing a built-in electric field (Fig. 8e). During sliding, the electrons will be excited and jump to the LUMO of the PEDOT by the released "bindington". Then the electrons and holes were driven by the built-in electric field, generating DC current (Fig. 8f). One PEDOT coated textile nanogenerator can generate 0.5 V open-circuit voltage and 12 μA short-circuit current by hand rubbing.

2D materials

2D materials exhibit many peculiar properties because their carrier migration and heat diffusion are confined to the two-dimensional plane. Their band gap tunable properties are widely used in fields such as field effect tubes, photoelectric devices, thermoelectric devices, *etc*. Compared with the surface of solid materials, the electronic structure of 2D materials is simpler

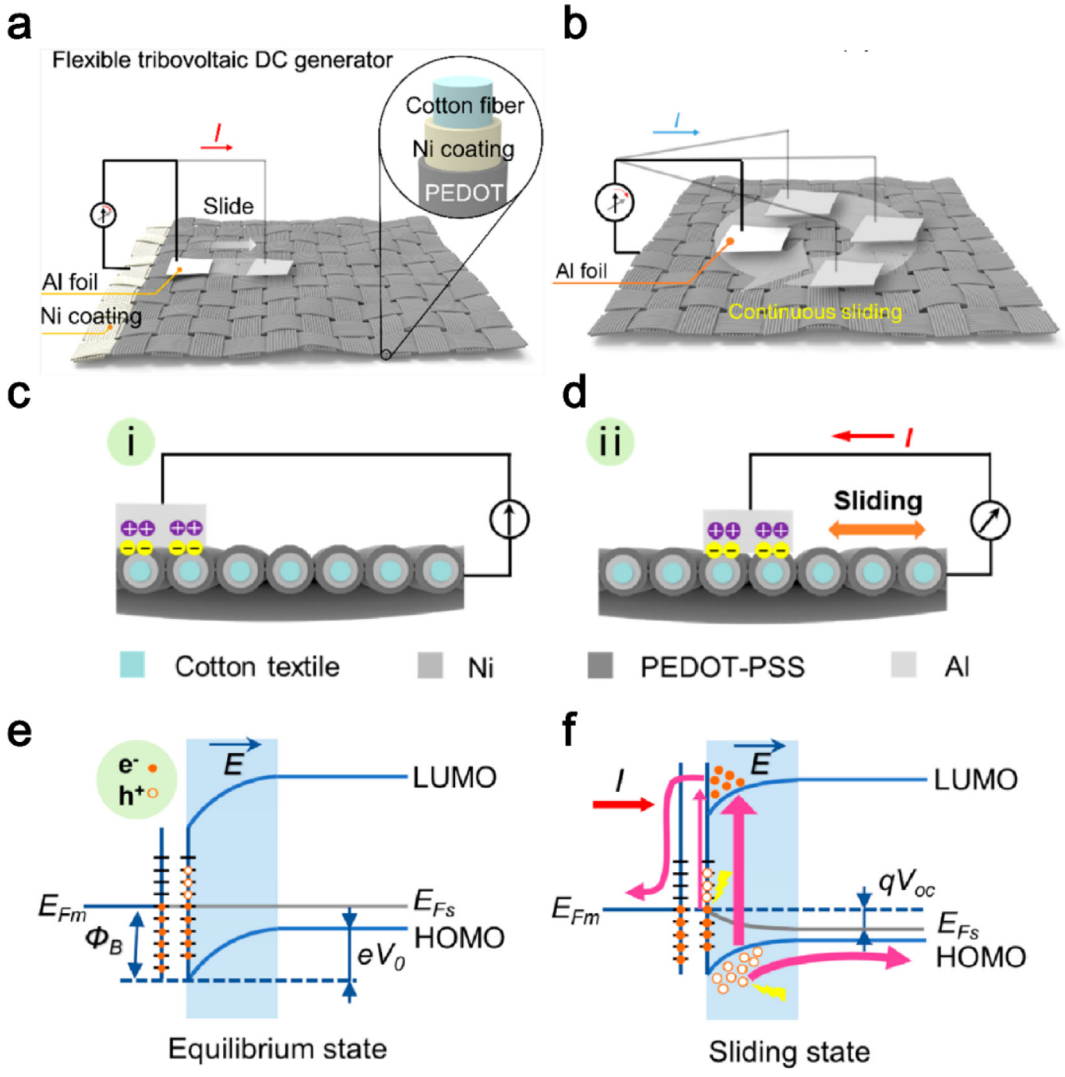

FIGURE 8

The textile tribovoltaic DC nanogenerator. (a) Schematic diagram of a textile tribovoltaic DC nanogenerator and (b) the experiment set up of generating of DC current. (c and d) The electricity generation process of the textile tribovoltaic nanogenerator. (e and f) Energy band diagram of the Al − PEDOT interface in the equilibrium state and sliding state, respectively [113].

Please cite this article in press as: S. Lin, Z. Lin Wang, Materials Today, (2022), https://doi.org/10.1016/j.mattod.2022.11.005

and clearer, and the study of the tribovoltaic effect of 2D materials has scientific significance.

MoS_2 and graphene are two 2D materials most commonly used in the study of the tribovoltaic effect. *Liu et al*. synthesized a thin MoS_2 film via PLD, and a conductive tip was used to slide against the MoS_2 film to generate tribo-current, which was found up to 10^6 A/m^{-2}(−|-) [24]. Further, they discussed the output of various sliding MoS_2 multilayer-based heterojunctions, as shown in Fig. 9a [76]. The results turned out that the band bending of MoS_2 played a dominate role in determining the direction of the tribo-current, which supported the mechanism of tribovoltaic effect. In addition to MoS_2, the tribovoltaic effect involving graphene was also investigated. However, due to the lack of relevant studies, no advantages have been found in the output performance of tribovoltaic nanogenerators composed of graphene. For example, according to You's report, the output performance of the PEDOT:PSS/graphene tribovoltaic nanogenerators is far worse than that of PEDOT:PSS/Al tribovoltaic nanogenerators, as shown in Fig. 9b [112]. But anyway, a graphene-based generator should have the advantage of low friction, since that the graphene is a good solid lubricating material [52].

Effect of contact electrification on tribovoltaic effect

The tribovoltaic effect occurs at sliding interfaces, in which semiconductors are involved. A highly related phenomenon, contact electrification, occurs at almost any sliding interface, including those involving semiconductors. In contact electrification, the electrons transfer from one surface to the other surface, and the net charges are generated when the two surfaces separate. The net charge at the interface will induce an electric field and establish a potential barrier, which may affect the generation of DC tribo-current induced by the tribovoltaic effect. Deng *et al*. first investigated the effects of surface charges on the charge pumping at the p-type and n-type semiconductors interface by using first-principle methods [115]. It was proposed that the surface charges can significantly affect the electric potential distribution in the depletion region, which hinders the transfer of electron and hole across the contact interface and further affect the charge pumping current. In other words, the surface charges have a negative impact on the transfer of electron and hole between two contacted semiconductor surfaces.

The mechanism of the tribovoltaic effect at the sliding semiconductor interface is different from the pumping current between two contact and separate semiconductors, which has been discussed in Section 3.2. Both current generations between two semiconductors in contact mode and sliding mode are both highly related to the charge barriers formed at the interface. And the surface charges induced by contact electrification have been demonstrated to modulate the interface potential distribution [115]. Therefore, the surface charge generated by contact electrification should also be able to influence the tribovoltaic effect in sliding mode. However, the contribution of the surface charges to the tribovoltaic effect was not considered until the third-generation semiconductors were used in the experiment, as shown in Fig. 9c and 9d [114]. In studies of the tribovoltaic effect, first-generation semiconductors such as silicon are usually used. Compared with the third-generation semiconductor, the first-generation semiconductor has a narrower band gap width and higher conductivity. The high conductivity of the first-generation semiconductor makes it difficult for triboelectric charges to be trapped on the surface, so that the effect of triboelectric charges on the tribovoltaic effect cannot be detected.

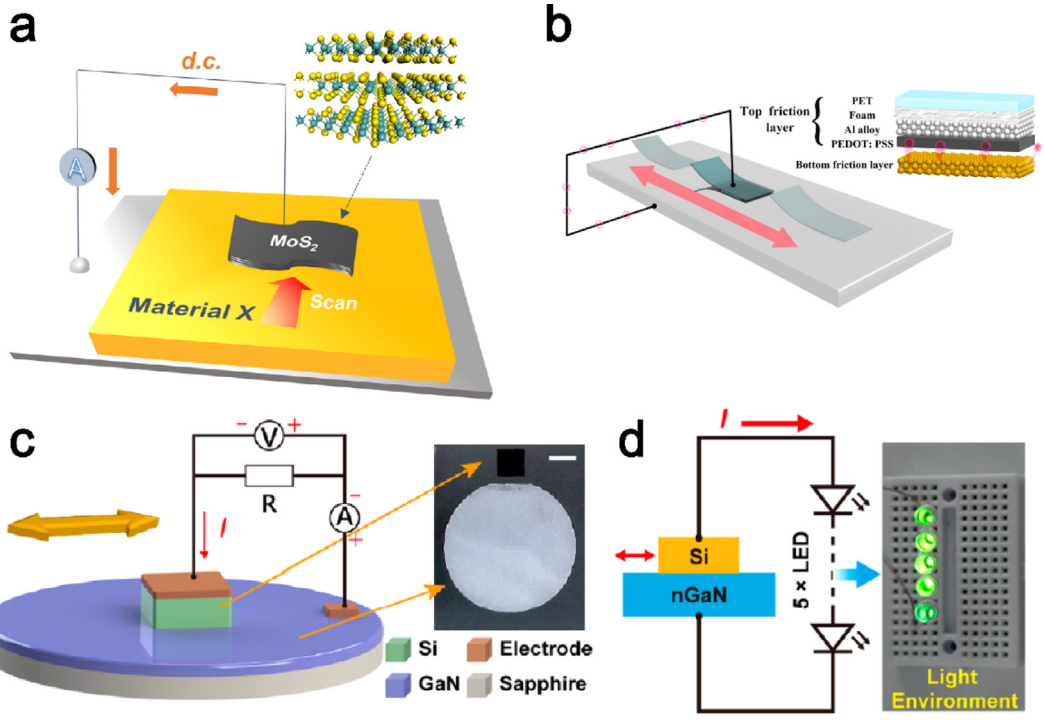

FIGURE 9

The tribovoltaic effect involving (a and b) 2D materials [76,112] and (c and d) third generation semiconductors [114].

Please cite this article in press as: S. Lin, Z. Lin Wang, Materials Today, (2022), https://doi.org/10.1016/j.mattod.2022.11.005

The third-generation semiconductors were introduced in the studies of the tribovoltaic effect because of their wide bandgap, which was expected to induce a higher tribo-voltage. Chen *et al*. investigated a series of gallium nitride (GaN) based tribovoltaic nanogenerators, including GaN-Si and GaN-Al. The maximum open circuit voltage of the tribovoltaic nanogenerator involving GaN reached 25 V, which was four times higher than the traditional tribovoltaic nanogenerator [114]. Further, the output tribo-voltage and tribo-current of GaN-based tribovoltaic nanogenerator were increased to 130 V and 340 μA, respectively [116]. Such a tribo-voltage was much higher than the strength of the built-in electric field. Unlike traditional tribovoltaic effect, it was revealed that the external tribo-current always flows from GaN side to the Si/Al side, instead of depending on the built-in electric field induced by the diffusion of charge carriers. This indicates that there are other driving forces to separate electron-hole pairs excited during friction, most likely the surface charges induced by contact electrification, since that the electric field generated by the static charges can reach several thousand volts [117,118].

Combined with contact electrification, Chen *et al*. proposed a model for explaining the tribovoltaic effect involving third-generation semiconductors [114]. As shown in Fig. 10a, the electrons belonging to Si and GaN are trapped in the Electron-cloud-potential-wells. When Si sliding on the GaN surface, the potential barrier for the transition of electrons is reduced and electrons transfer from Si surface to the GaN surface due to the high energy level of Si (Fig. 10b). Increasing the friction strength, more electrons will transfer from Si side to the GaN side, as shown in Fig. 10c. Assuming that the Fermi level of the n-type GaN is higher than that of Si (Fig. 10d), the electrons will diffuse from GaN side to the Si side when they come into contact (Fig. 10e), and establish a built-in electric field point from GaN side to the Si side. The stronger friction, the stronger built-in electric field at the interface (Fig. 10f). It was noticed that the direction of electron transfer in contact electrification was opposite to that caused by diffusion induced by electron concentration difference. In the third-generation semiconductor tribovoltaic effect, the electric field induced by the contact electrification plays a dominate role, and the direction of the external tribo-current flowed from GaN side to Si side. Introducing third-generation and triboelectric surface charges to the tribovoltaic effect provides a new idea for the development of high-performance tribovoltaic nanogenerators.

Hybrid tribovoltaic generator

As a generator, how to improve its output performance is a key problem. In the research of traditional TENG, the output performance of hybrid TENG can be significantly improved by collecting both triboelectric charges induced current and other forms of energy, such as the current generated by electromagnetic induction [119,120] and solar energy [121,122], *etc*. It was also demonstrated that designing hybrid tribovoltaic nanogenerator is a good strategy to improve the output performance of the tribovoltaic nanogenerators [68,71,125–129]. For hybrid generators, the collected target energy should ideally be complementary. For example, a generator that collects solar and mechanical

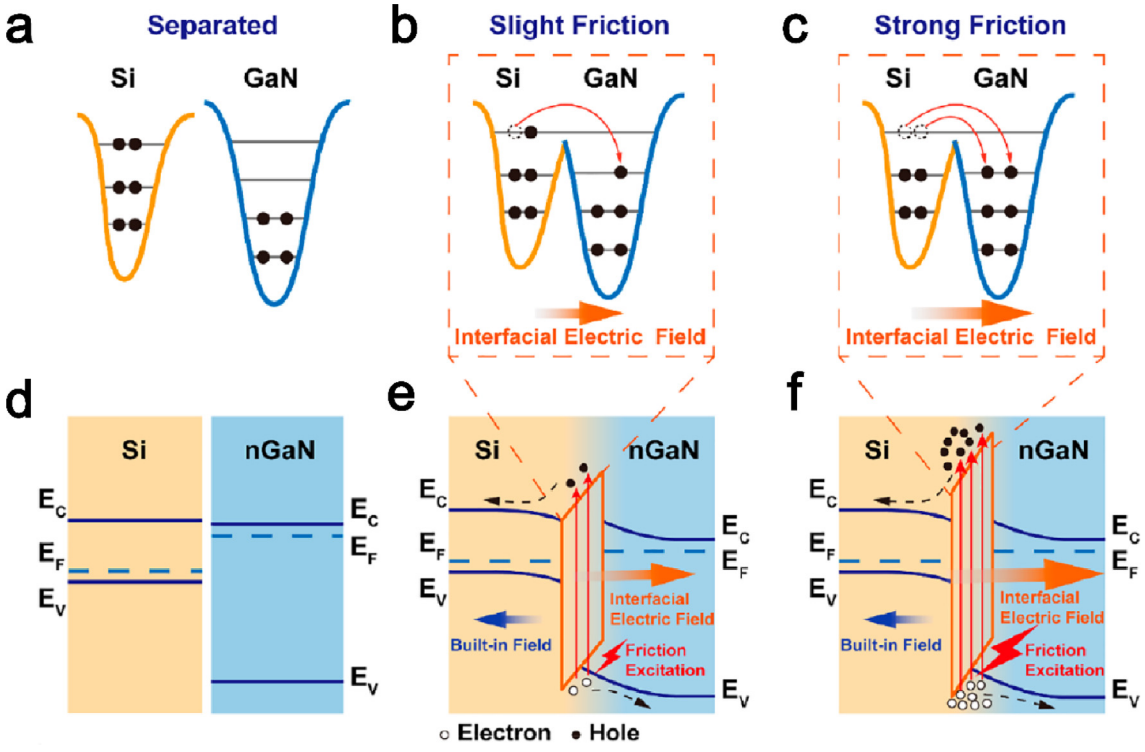

FIGURE 10

Contribution of charge transfer induced by contact electrification to the tribovoltaic effect. Electron-cloud-potential-well model for contact electrification between GaN and Si (a) in separated state, (b) slight friction state, and (c) strong friction state. Band diagram of Si and nGaN (d) in separated state, (e) slight friction state, and (f) strong friction state [114].

Please cite this article in press as: S. Lin, Z. Lin Wang, Materials Today, (2022), https://doi.org/10.1016/j.mattod.2022.11.005

energy works perfectly on sunny days, while mechanical energy provides most of the energy supply on cloudy days. For a tribovoltaic nanogenerator, it should instinctively be able to absorb solar energy because its interface electronic structure is not fundamentally different from that of a photovoltaic generator, and a stationary tribovoltaic generator may be taken as a photovoltaic generator. Therefore, most hybrid tribovoltaic nanogenerators currently capture both solar and mechanical energy, as shown in Fig. 11a [128]. The only difference between the hybrid tribovoltaic-photovoltaic nanogenerator and the ordinary tribovoltaic nanogenerator is that the light can reach the sliding interface in the hybrid tribovoltaic-photovoltaic nanogenerator.

Hao *et al*. investigated the dynamic metal/perovskite Schottky junction under light illumination [129]. It was found that the light illumination can increase the tribo-current between metal and the perovskite significantly. In a dark environment, the tribo-voltage and tribo-current density between Al and perovskite were 0.7 V and 41.1 A/m^2, respectively. Under light illumination, the output current density was increased by 3-fold compared to that in the dark environment. Ren *et al*. used an UV light to illuminate a sliding Si-GaN interface, the tribo-current was found to increase 13 times and the tribo-voltage increase 4 times under UV light irradiation [128]. The mechanism of hybrid tribovoltaic-photovoltaic nanogenerator seems easy to understand. It was pointed out that the light irradiation could excite photogenerated carriers, which increases the concentration of electron-hole pairs at the interface, leading to an increase in the output current and voltage under the light irradiation. However, it was noticed that at some semiconductor interfaces, such as those between DI water and silicon, illumination can produce a constant background photocurrent that sliding is not required [32]. The result is like a simple linear superposition of the photovoltaic effect and tribovoltaic effect. At some interfaces, such as silicon and GaN, light irradiation increases

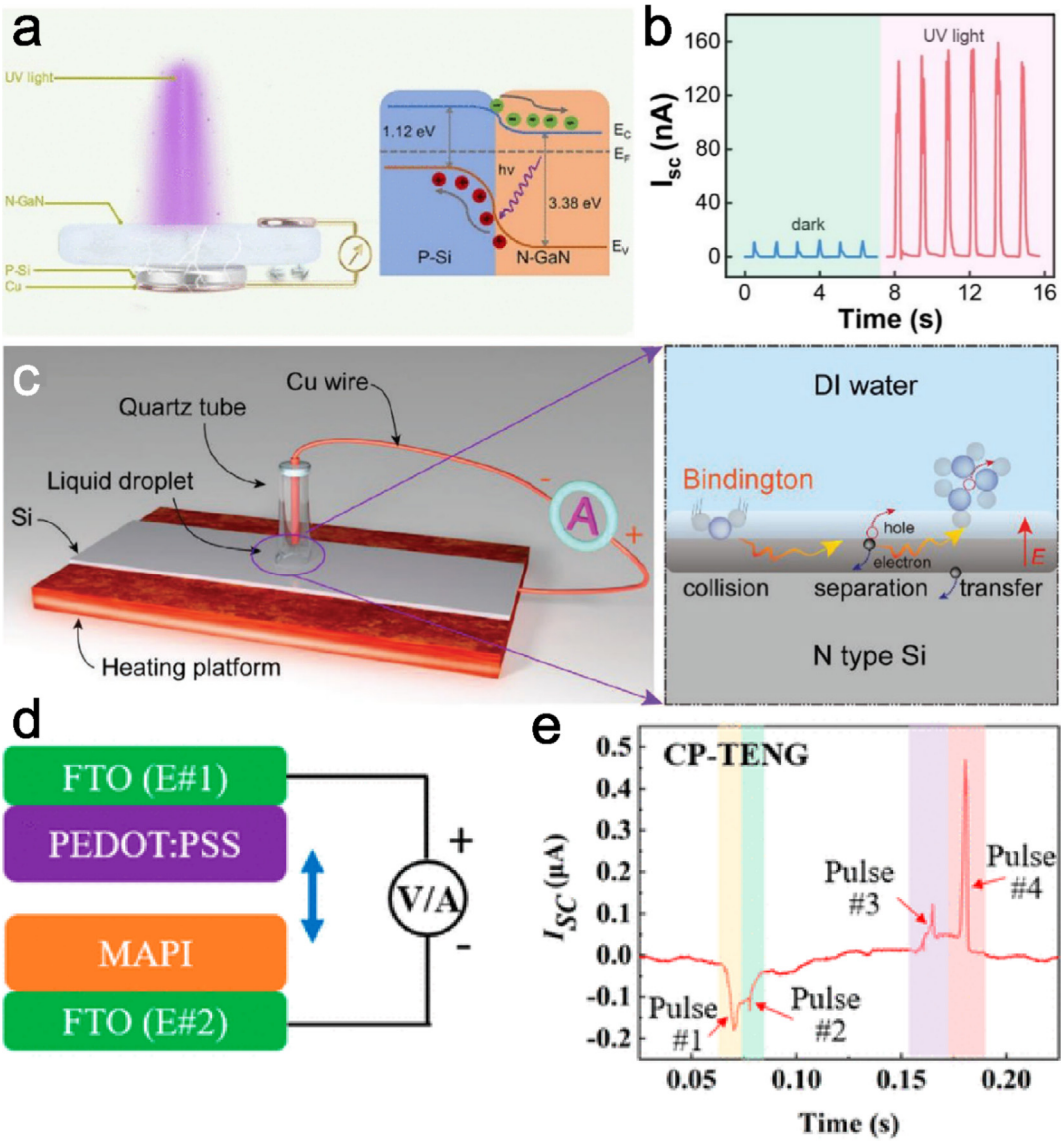

FIGURE 11

Hybrid tribovoltaic nanogenerators. (a and b) Increasing the output of the tribovoltaic nanogenerator by UV irradiation [128]. (c) Effect of temperature on the tribovoltaic effect at DI water and silicon interface [31]. (d and e) The semiconductor contact-separation TENG and its output current [130].

Please cite this article in press as: S. Lin, Z. Lin Wang, Materials Today, (2022), https://doi.org/10.1016/j.mattod.2022.11.005

the tribo-current without creating a background current, as shown in Fig. 11b [128]. The difference of these two phenomena remains to be further explained.

Another way to increase the carrier concentration at the interface is to increase the temperature. As introduced in Section 2.3, new chemical bonds will form at the interface owing to the collisions of the molecules, releasing "bindington" and exciting electron-hole pairs. As temperature rises, molecules collide more violently with each other, forming new chemical bonds more easily and releasing more "bindington", which in turn increases the concentration of electron-hole pairs at the interface and raises the tribovoltaic current. According to this analysis, Zheng *et al*. discussed the effect of temperature on the tribovoltaic effect, and it was revealed that both the tribovoltaic current and voltage at the DI water-Si interface increased with the increasing temperature, as shown in Fig. 11c [31]. This research provides an idea to develop a hybrid tribovoltaic nanogenerator capable of harvesting thermal and mechanical energy.

TENG and tribovoltaic nanogenerator have a common feature, which is that they generally have sliding interface or contact-separation interface, which provides the possibility to collect both triboelectric induced current and tribovoltaic current at the same time. Wang *et al*. investigated the output current between two contact-separation semiconductors, as shown in Fig. 11d and 11e [130]. The results indicated that the current signal of the semiconductor contact-separation TENG comes from two sources. One part is generated by the electron transfer in CE and the electrostatic induction, as that occurs in traditional TENGs, and the other part is the electron transfer pumped by the PN junction. Similarly, if the semiconductor materials are used in the sliding mode TENG, both electrostatic induction and tribovoltaic effect will contribute to the tribo-current, and it can be regarded as a hybrid generator consisting of a TENG and a tribovoltaic nanogenerator.

Applications based on tribovoltaic effect

The tribovoltaic effect is a newly discovered phenomenon. Although the tribovoltaic effect has been applied to harvest energy and design sensor, compared with the traditional TENG, the application research of tribovoltaic effect is in the preliminary stage. In fact, the use of tribovoltaic nanogenerators as energy harvesting devices has the advantage of direct DC output. They are usually designed by introducing the semiconductor materials at a sliding interface so that sliding occurs at the semiconductor interface to generate tribovoltaic current as shown in Fig. 12a. The forces that drive the interface to slide can be a variety of mechanical powers, such as wind power, water power and human power *etc*. For example, Yu *et al*. designed a tribovoltaic nanogenerator that can be driven by the wind, and can produce 4.4 mA tribovoltaic current [131]. The tribovoltaic effect is demonstrated to be sensitive to many friction parameters, such as sliding speed and sliding load [106]. Based on the relations between the tribovoltaic output current and the friction parameters, different sensors can be designed. Siliding is a necessary condition for the generation of the tribovoltaic effect. Tribovoltaic current can only be generated only when two semiconductors have relative siliding, which can be used to detect whether the two objects have relative motion. By integrating the tribovoltaic current, the relative displacement of the objects can be obtained, which can be used as a position sensor, as shown in Fig. 12b. Furthermore, it was reported that the tribovoltaic current between water and fluorinated graphite was proportional to the relative velocity between them [82]. And the fluorinted graphite based tribovoltaic nanogenerator was designed to detect the water speed.

In addition to being an energy harvester and smart sensor, the tribovoltaic nanogenerator may also serve as a new data storage technique. As we know, the electron transfer at the ferromagnet interfaces is spin dependent [132,133]. When the magnetization direction of adjacent ferromagnet films is the same, the whole interface shows a low resistance state; conversely, when the magnetization direction of adjacent ferromagnet films is opposite, the whole interface shows a high resistance state, which is referred to as the giant magnetoresistance effect [134,135]. If using magnetic semiconductor materials as sliding pair, the tribovoltaic current is likely to be affected by the magnetization direction of the two sliding materials. A reasonable assumption is that when the direction of magnetization of the two is the same, sliding interface can generate a larger current compared to that generated in the condition when the direction of magnetization of the two is opposite. If this assumption is confirmed, it is possible to store data by magnetizing semiconductor ferromagnets, as shown in Fig. 12c. Because the tribovoltaic current also depends on the semiconductor properties, such as the doping concentration, and resistance [69,85], therefore, the tribovoltaic effect can also be used to characterize the material properties at microscale, as shown in Fig. 12d.

Conclusion and perspectives

In this review, we have summarized recent works on the tribovoltaic effect and clearly introduced the mechanism of the tribovoltaic effect. At the sliding semiconductor interface, the formation of new bonds will release energy quantum, named "bindington", which excites the electron-hole pairs at the interface. The electron-hole pairs are further separated by the built-in electric field, generating a DC tribo-current.

The tribovoltaic effect at different sliding interfaces, including metal–semiconductor interface, P—N junction, metal–insulator-semiconductor, metal–insulator-metal and liquid-semiconductor interface, was discussed. When the insulator layer was introduced at the interface, the excited electrons will tunnel through the insulator layer when it is thin (several nanometers). If the insulator layer is thick, the thermionic emission and defect conduction will contribute to the tribovoltaic current.

The tribovoltaic effect was demonstrated to be affected by the surface properties of the semiconductors. It was shown that the surface state density of semiconductor, the strength of the built-in electric field and the interaction between two surfaces can be changed by surface modification, and then the tribovoltaic effect can be modulated. Moreover, by selecting materials with special functions, such as flexible materials, the tribovoltaic effect can be applied to corresponding situations. In particular, if third-generation semiconductors are involved in sliding, the contribution of the electric field induced by the triboelectric charges at the interface to the tribovoltaic effect is significant.

Please cite this article in press as: S. Lin, Z. Lin Wang, Materials Today, (2022), https://doi.org/10.1016/j.mattod.2022.11.005

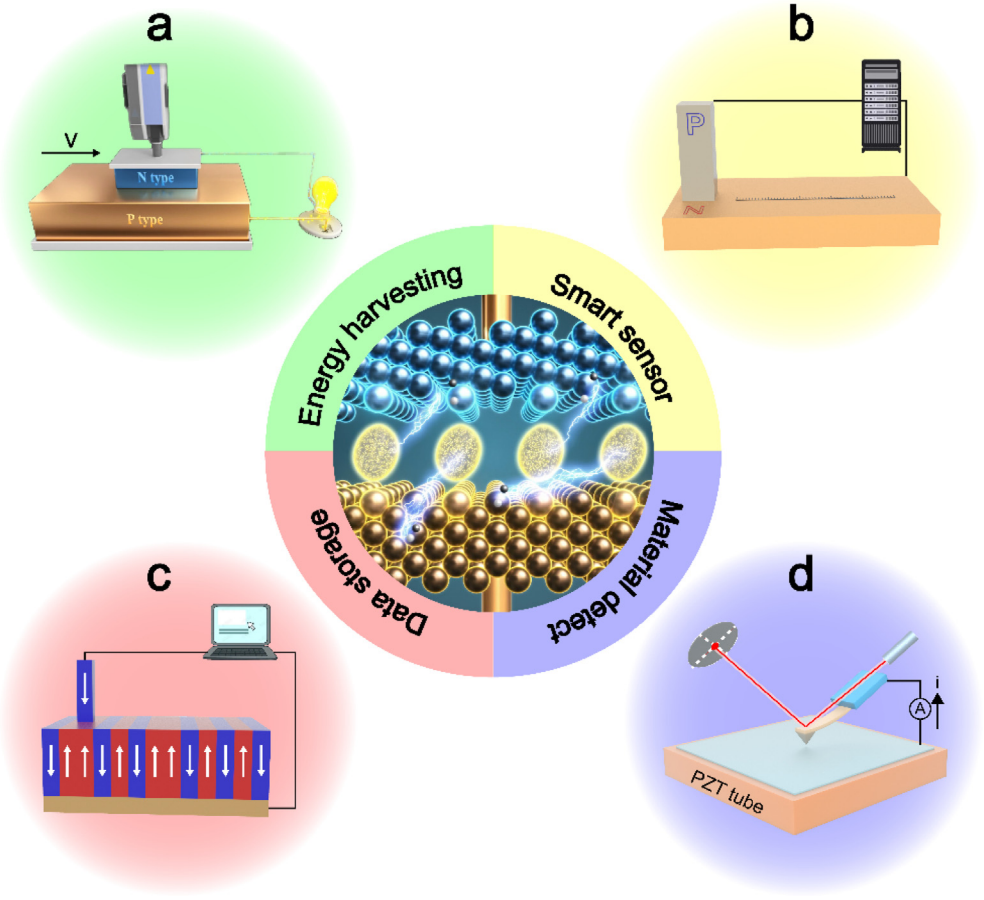

FIGURE 12

Poential applications of tribovoltaic effect. Tribovoltaic nanogenerator for (a) energy harvesting, (b) smart sensor, (c) data storage and (d) material characterization [69].

In order to increase the output power of the tribovoltaic nanogenerator, hybrid tribovoltaic nanogenerator was proposed to harvest the tribovoltaic current and other forms of energy, such as solar energy and thermal energy. In addition to harvesting energy, tribovoltaic nanogenerators have also been shown to be able to be used as self-powered sensors.

Compared with the photovoltaic effect, the tribovoltaic effect is only just being discovered. Although tribovoltaic effect has been shown to widely occur at various semiconductor material interfaces, it has not been discussed in depth. Here are the challenges to be investigated (and the roadmap for tribovoltaic effect is shown in Fig. 13):

1. Fundamental theory and in-depth mechanism of the tribovoltaic effect. From the theoretical point of view, the "bindington" that excites electron-hole pairs specific is released by chemical bond formation, but how to modulate the energy of the "bindington" by controlling interface chemical reaction remains to be future investigated. Quantum mechanical theory has to be established as well as carrier transport theory have to be established for quantitative understanding the tribovoltaic effect.
2. Choice of materials for enhanced tribovoltaic effect. The current study discussed the effect of conductivity, doping concentration, *etc*. of semiconductors on the tribovoltaic effect. However, there are many properties of materials, such as modulus of elasticity, hardness, heat capacity, thermal conductivity, *etc*., that need to be investigated. Based on the fact that material properties affect the tribovoltaic effect, a set of guidelines for the selection of semiconductor materials for tribovoltaic nanogenerator needs to be developed to enhance the tribovoltaic effect.
3. Environment effects on the tribovoltaic effect. In addition to material properties, friction conditions, such as sliding speed, sliding load, sliding frequency, *etc*., as well as environmental conditions, such as temperature, humidity, atmosphere, *etc*., may affect the tribovoltaic effect.
4. Contact electrification enhanced tribovoltaic effect. Contact electrification has been shown to affect the tribovoltaic effect. The electric field formed by the interfacial triboelectric charges is much lager than the built-in electric field at the semiconductor interface. Therefore, increasing the triboelectric charge density at the sliding semiconductor interface is an effective strategy to enhance the tribovoltaic effect. The method of increasing the triboelectric charges at the semiconductor interface can be borrowed from traditional TENG, such as using charge pumping technology, applying bias and so on.
5. Applications of tribovoltaic effect. In terms of application research, the development of tribovoltaic nanogenerators is just beginning and there is very little relevant literature avail-

Please cite this article in press as: S. Lin, Z. Lin Wang, Materials Today, (2022), https://doi.org/10.1016/j.mattod.2022.11.005

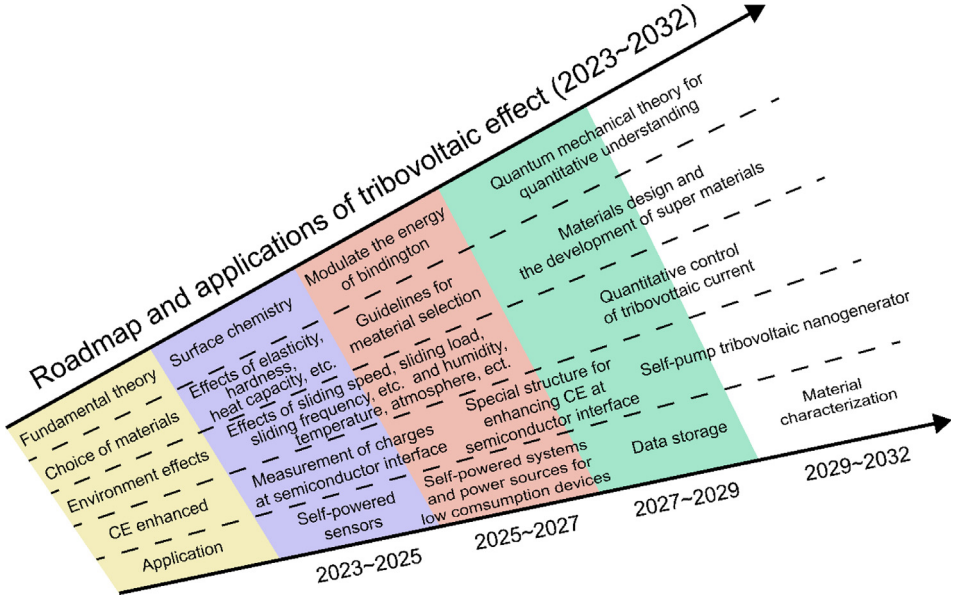

FIGURE 13

Proposed technology roadmap for tribovoltaic effect.

able now. How to use the tribovoltaic nanogenerator in various applications in the future, such as power sources and self-powered sensors, is also a key point needed to be discussed.

Data availability

Data will be made available on request.

Declaration of Competing Interest

The authors declare that they have no known competing financial interests or personal relationships that could have appeared to influence the work reported in this paper.

Acknowledgements

This work was supported by the National Natural Science Foundation of China (Grant No. 52192610), and National Key R & D Project from Minister of Science and Technology (2021YFA1201601).

References

[1] Z.L. Wang, Nano Energy 58 (1989) 669–672.
[2] Y. Yang, Z.L. Wang, Iscience 24 (2021) 102358.
[3] F. Fan, Z.L. Wang, Nano Energy 1 (2012) 328–334.
[4] C. Wu et al., Adv. Energy Mater. 9 (2019) 1802906.
[5] Y. Zhou et al., Nano Energy 84 (2021) 105887.
[6] L. Cheng et al., Nat. Commun. 9 (2018) 3773.
[7] Z. Bai et al., Nano Energy 94 (2022) 106956.
[8] J. Zhu et al., EcoMat 2 (2020) e12058.
[9] H. Wang et al., Nano Energy 78 (2020) 105241.
[10] J. Zhu et al., Nano Energy 73 (2020) 104760.
[11] Y. Xie et al., Adv. Mater. 26 (2014) 6599–6607.
[12] Y. Yang et al., Adv. Mater. 25 (2013) 6594–6601.
[13] J. Kim et al., Adv. Energy Mater. 10 (2020) 2002312.
[14] W. Cao et al., Adv. Funct. Mater. 30 (2020) 2004181.
[15] F. Xing et al., Nano Energy 42 (2017) 138–142.
[16] N. Cui et al., ACS Appl. Mater. Interfaces 7 (2015) 18225–18230.
[17] L. He et al., ACS Nano 16 (2022) 6244–6254.
[18] B. Chen, Y. Yang, Z.L. Wang, Adv. Energy Mater. 8 (2018) 1702649.
[19] Z. Lin et al., Angew. Chem. Int. Edit. 52 (2013) 12545–12549.
[20] X. Yang et al., Nano Energy 44 (2018) 388–398.
[21] G. Qiao et al., Nano Energy 79 (2021) 105408.
[22] Y. Zi et al., Nat. Commun. 7 (2016) 10987.
[23] Y. Song et al., Adv. Energy Mater. 10 (2020) 2002756.
[24] J. Liu et al., Nat. Nanotechnol. 13 (2018) 112–116.
[25] Z.L. Wang, A.C. Wang, Mater. Today 30 (2019) 34–51.
[26] R. Yang et al., Nano Energy 83 (2021) 105849.
[27] W. Chen, A. Andreev, L. Glazman, Phys. Rev. Lett. 106 (2011) 216801.
[28] M. Buscema et al., Nat. Commun. 5 (2014) 4651.
[29] L. Su, W. Yang, J. Cai, H. Chen, X. Feng, Small 13 (2017) 1701687.
[30] Y. Dou et al., Chem. Commun. 58 (2022) 8548–8551.
[31] M. Zheng et al., Adv. Mater. Interfaces 9 (2022) 2101757.
[32] M. Zheng et al., Nano Energy 83 (2021) 105810.
[33] S. Lin, X. Chen, Z.L. Wang, Chem. Rev. 122 (2022) 5209–5232.
[34] Q. Dong et al., Science 347 (2015) 967–970.
[35] G. Dennler, M. Scharber, C. Brabec, Adv. Mater. 21 (2009) 1323–1338.
[36] Y. Li, Accounts Chem. Res. 45 (2012) 723–733.
[37] P. Landsberg, Solid State Electronics 18 (1975) 1043–1052.
[38] M. Archer, Phys. E 14 (2002) 61–64.
[39] B. Parida, S. Iniyan, R. Goic, Renew. Sust. Energy Rev. 15 (2011) 1652–11636.
[40] L. Kronik, Y. Shapira, Surf. Sci. Rep. 37 (1999) 1–206.
[41] K. Holmberg, A. Erdemir, Friction 5 (2017) 263–284.
[42] H. Sakuma et al., Sci. Adv. 4 (2018) eaav2268.
[43] J. Krim, Am. J. Phys. 70 (2002) 890.
[44] J. Luo, M. Liu, L. Ma, Nano Energy 86 (2021) 106092.
[45] M. Jean, Comput. Method Appl. M. 177 (1999) 235–257.
[46] M. Raous, L. Cangemi, M. Cocu, Comput. Method Appl. M. 177 (1999) 383–399.
[47] Z. Zhang, X. Shi, D. Guo, Math. Probl. Eng. 2016 (2016) 6530213.
[48] , Clarendon Press, Oxford, 1964.
[49] G. Sutter, N. Ranc, Wear 268 (2010) 1237–1242.
[50] B. Perssion, J. Phys: Condens. Matter. 18 (2006) 7789–7823.
[51] G. Liu, J. Liu, W. Dou, Nano Energy 96 (2022) 107034.
[52] X. Huang et al., Nat. Commun. 12 (2021) 2268.
[53] I. Sivebaek, B. Persson, Tribol. Lett. 62 (2016) 5.
[54] K. Kristiansen et al., Adv. Funct. Mater. 21 (2011) 4555–4564.
[55] Z. Xu, P. Huang, Acta Phys. *Sin-ch Ed.* 55 (2006) 2427–2432.
[56] Z. Xu, P. Huang, Wear 262 (2007) 972–977.
[57] K. Nakayama, H. Hashimoto, Tribol. Int. 29 (1996) 385–393.
[58] M. Zheng et al., Theor. Appl. Fract. Mec. 32 (1999) 75–80.
[59] K. Tian et al., ACS Nano 13 (2019) 7425–7434.
[60] M. Srinivasan, Phys. Rev. E 80 (2009) 046124.
[61] A. Filippov, J. Klafter, M. Urbakh, Phys. Rev. Lett. 92 (2004) 135503.

Please cite this article in press as: S. Lin, Z. Lin Wang, Materials Today, (2022), https://doi.org/10.1016/j.mattod.2022.11.005

[62] K. Tian et al., Phys. Rev. Lett. 118 (2017) 076103.
[63] J. Batteas, X. Quan, M. Weldon, Tribol. Lett. 7 (1999) 121–128.
[64] J. Batteas, M. Weldon, K. Raghavachari, Nanotribology Crit. Assess. Futur. Res. Needs (2003) 387–398.
[65] A. Li, Y. Liu, I. Szlufarska, Tribol. Lett. 56 (2014) 481–490.
[66] H. Shao et al., Adv. Mater. 28 (2016) 1461–1466.
[67] H. Zheng et al., Adv. Funct. Mater. 31 (2021) 2105325.
[68] J. Han et al., Nano Energy 58 (2019) 331–337.
[69] M. Zheng et al., Adv. Mater. 32 (2020) 2000928.
[70] S. Lin et al., Adv. Sci. 6 (2019) 1901925.
[71] Z. Zhang et al., Mater. Today Phys. 16 (2021) 100295.
[72] Y. Lu et al., iScience 22 (2019) 58–69.
[73] R. Xu et al., Nano Energy 66 (2019) 104185.
[74] Q. Zhang, R. Xu, W. Cai, Nano Energy 51 (2018) 698–703.
[75] Y. Lu et al., Research 2019 (2019) 5832382.
[76] J. Liu et al., ACS Appl. Mater. Interfaces 11 (2019) 35404–35409.
[77] S. Deng et al., Nano Energy 94 (2022) 106888.
[78] J. Liu et al., Mater. Horiz. (2019) 6 1020.
[79] J. Liu et al., Nano Energy 48 (2018) 320–326.
[80] M. Benner et al., ACS Appl. Mater. Interfaces 14 (2022) 2968–2978.
[81] Y. Yan et al., J. Phys. Chem. C 125 (2021) 14180–14187.
[82] H. Huang, R. Wang, Y. Chen, Nano Energy 93 (2022) 106887.
[83] H. Zhong et al., Adv. Funct. Mater. 27 (2017) 1604226.
[84] Y. Lu et al., Research 2021 (2021) 7505638.
[85] S. Lin, X. Chen, Z.L. Wang, Nano Energy 76 (2020) 105070.
[86] Z. Lin et al., Adv. Mater. 26 (2014) 4690–4696.
[87] X. Liu et al., Nano Energy 66 (2019) 104188.
[88] G. Cheng et al., ACS Nano 8 (2014) 1932–1939.
[89] G. Zhu et al., ACS Nano 8 (2014) 6031–6037.
[90] L. Pan et al., Nano Research 11 (2018) 4062–4073.
[91] X. Li et al., Adv. Energy Mater. 8 (2018) 1800705.
[92] C. Le et al., Nano Energy 80 (2021) 105571.
[93] M. Xu et al., Nano Energy 57 (2019) 574–580.
[94] H. Cho et al., Nano Energy 56 (2019) 56–64.
[95] Z. Lin et al., Angew. Chem. Int. Ed. 52 (2013) 12545–12549.
[96] J. Ha et al., Nano Energy 36 (2017) 126–133.
[97] A.W. Copeland, O.D. Black, A.B. Garrett, Chem. Rev. 31 (1942) 177–226.
[98] F. Williams, A.J. Nozik, Nature 312 (1984) 21–27.
[99] N.S. Lewis, J. Phys. Chem. B. 102 (1998) 4843–4855.
[100] A. Iqbal, M.S. Hossain, K.H. Bevan, Phys. Chem. Chem. Phys. 18 (2016) 29466–29477.
[101] J. Liu et al., Adv. Electron. Mater. 5 (2019) 1900464.
[102] Y. Yu, X. Wang, Extreme Mech. Lett. 9 (2016) 514–530.
[103] Y. Feng et al., Nano Energy 19 (2016) 48–57.
[104] S. Ferrie et al., Nano Energy 78 (2020) 105210.
[105] S. Ferrie et al., Nano Energy 93 (2022) 106861.
[106] D. Yang et al., Nano Energy 99 (2022) 107370.
[107] L. Zhang et al., Matter 5 (2022) 1532–2546.
[108] J. Gao et al., J. Mater. Chem. A 9 (2021) 8950–8965.
[109] Q. Huang, D. Wang, Z. Zheng, Adv. Energy Mater. 6 (2016) 1600783.
[110] K. Keum et al., Adv. Mater. 32 (2020) 2002180.
[111] R. Yang et al., Adv. Funct. Mater. 31 (2021) 2103132.
[112] Z. You et al., Nano Energy 91 (2022) 106667.
[113] J. Meng et al., ACS Energy Lett. 6 (2021) 2442–2450.
[114] Y. Chen et al., ACS Appl. Mater. Interfaces 14 (2022) 24020–24027.
[115] S. Deng et al., Nano Energy 78 (2020) 105287.
[116] Z. Wang et al., Energy Environ. Sci. 15 (2022) 2366.
[117] F. Liu et al., Nano Energy 56 (2019) 482–493.
[118] Q. Zheng et al., Nano Energy 97 (2022) 107183.
[119] H. Guo et al., Adv. Energy Mater. 6 (2016) 1501593.
[120] X. Cui, S. Cao, H. Zhang, Energy Sci. Engineering 8 (2020) 574–581.
[121] S. Jeon, D. Kim, Y. Choi, Nano Energy 12 (2015) 636–645.
[122] D. Yoo et al., Nano Energy 57 (2019) 424–431.
[123] C. Ma et al., Energy Environ. Sci. 14 (2021) 374.
[124] H. Zhong et al., Carbon 105 (2016) 199–204.
[125] X. Xu et al., J. Mater. Sci. 55 (2020) 9014–9026.
[126] V. Sharov et al., ACS Appl. Energy Mater. 2 (2019) 4395–4401.
[127] J. Liu et al., Matter 1 (2019) 650–660.
[128] L. Ren et al., Nano Lett. 21 (2021) 10099–10106.
[129] Z. Hao et al., Matter 1 (2019) 639–649.
[130] H. Wang et al., ACS Appl. Mater. Interfaces (2022), https://doi.org/10.1021/acsami.2c06374.
[131] X. Yu et al., RSC Adv. 11 (2021) 19106.
[132] H. Reittu, J. Phys. Condensed Matter 9 (1997) 10651–10660.
[133] F. Blobner et al., Phys. Rev. Lett. 112 (2014) 086801.
[134] H. Saarikpski, W. Wetzels, G. Bauer, Phys. Rev. B 75 (2007) 075313.
[135] F. Mancoff et al., Appl. Phys. Lett. 88 (2006) 112507.

Please cite this article in press as: S. Lin, Z. Lin Wang, Materials Today, (2022), https://doi.org/10.1016/j.mattod.2022.11.005